

Approach to parton equilibration *

Xin-Nian Wang

Nuclear Science Division, MS70A-3307, Lawrence Berkeley Laboratory
University of California, Berkeley, CA 94720

Perturbative QCD-based models of parton production and equilibration in ultrarelativistic heavy ion collisions are reviewed with an emphasis on the treatment of quantum interference effects. Uncertainties in the initial parton production and their effects on later parton equilibration are considered. Probes of early parton dynamics are also discussed.

1. INTRODUCTION

In the last few years, there have been enormous new interests in a perturbative QCD-inspired description of ultrarelativistic heavy ion collisions based on the parton model [1]. The main argument for such a treatment of high-energy heavy ion collisions lies in the nuclear structure at different scales. When the transverse momentum transfer involved in each nucleon-nucleon collision is small, $p_T \lesssim \Lambda_{\text{QCD}}$, effective models based on, *e.g.*, meson-exchange and resonance formation are sufficient to describe multiple interactions between hadrons, in which parton structure of the hadrons cannot yet be resolved. Those coherent (with respect to partons inside a hadron) interactions lead to collective behaviors in low and intermediate energy heavy ion collisions as first observed in Bevalac experiments [2] and recently in experiments at the AGS energy [3]. However, when p_T becomes large enough to resolve individual partons inside a nucleon, the dynamics is best described on the parton level via perturbative QCD (pQCD). Though hard parton interactions occur at CERN-SPS energies ($\sqrt{s} \lesssim 20$ AGeV), they play a negligible role in the global features of heavy ion collisions. However, at collider energies ($\sqrt{s} \gtrsim 100$ AGeV) the importance of hard or semihard parton scatterings is clearly seen in high-energy pp and $p\bar{p}$ collisions [4]. They are therefore also expected to be dominant in heavy ion collisions at RHIC and LHC energies [5, 6].

Hard or semihard interactions happen in a very short time scale and they generally break color coherence inside an individual nucleon. After the fast beam partons pass through each other and leave the central region, a dense partonic system will be left behind which is not immediately in thermal and chemical equilibrium. Partons inside such a system will then further interact with each other and equilibration will eventually be established if the interaction is frequent enough among the sufficiently large number of initially produced partons. Due to the asymptotic behavior of QCD, production rates of hard and semihard partons are calculable via pQCD during the initial stage of heavy

*This work was supported by the Director, Office of Energy Research, Division of Nuclear Physics of the Office of High Energy and Nuclear Physics of the U.S. Department of Energy under Contract Nos. DE-AC03-76SF00098, and by the U.S.-Hungarian Science and Technology Joint Fund J.F.No.378.

ion collisions. The color screening mechanism in the initially produced dense partonic system may make it also possible to use pQCD to investigate the thermal and chemical equilibration of the system. In this talk, I will give a brief review of parton production in high energy heavy ion collisions. Then I will concentrate on recent developments in early parton dynamics. I will also discuss the uncertainties in the initial condition of parton equilibration and their consequences in the formation of a quark-gluon plasma.

2. INITIAL PARTON PRODUCTION

In a parton model, a nucleus can be considered as an assemble of interacting partons. Because of vacuum fluctuations, a valence quark can radiate many off-shell gluons, quarks and antiquarks. These partons, if undisturbed, will reassemble back to the valence quark. However, a hard scattering can break the coherence and bring these virtual partons on shell. The parton number density $f_{a/A}(x, Q^2)$ thus depends on the resolution of the probe or the momentum transfer Q^2 of the collision. Similarly, a hard scattering can also lead to final state radiations off the scattered partons which can be described by fragmentation functions $D_{a/b}(z, Q^2)$. In the leading logarithmic approximation in an axial gauge, the interference between multiple radiations and between initial and final state radiations can be neglected. The amplitude for successive radiations then has a simple ladder structure and both the parton distribution functions $f_{a/A}(x, Q^2)$ and the fragmentation functions follow the Altarelli-Parisi evolution equations [7] with respect to Q^2 .

Using the parton distribution functions $f_{a/A}(x, Q^2)$, parton scattering rates in nucleus-nucleus collisions can be written as

$$\frac{dN_{jet}(b)}{dp_T^2 dy_1 dy_2} = K \int d^2\mathbf{r} \sum_{a,b} x_1 f_{a/A}(x_1, p_T^2, \mathbf{r}) x_2 f_{b/B}(x_2, p_T^2, \mathbf{b} - \mathbf{r}) \frac{d\sigma_{ab}}{d\hat{t}}, \quad (1)$$

where $d\sigma_{ab}$ is the cross section for parton-parton scatterings, y_1 and y_2 are the rapidities of the scattered partons, x_1 and x_2 are the light-cone momentum fractions carried by the initial partons, and the summation runs over all parton species. The factor $K \approx 2$ accounts for next-to-leading order effects. The parton distribution density of a nucleus is,

$$f_{a/A}(x, Q^2, \mathbf{r}) = t_A(\mathbf{r}) S_{a/A}(x, \mathbf{r}) f_{a/N}(x, Q^2), \quad (2)$$

where $t_A(\mathbf{r})$ is the thickness of the nucleus which is normalized to $\int d^2\mathbf{r} t_A(\mathbf{r}) = A$, $f_{a/N}(x, Q^2)$ is the parton structure function of a nucleon and $S_{a/A}(x, \mathbf{r})$ accounts for the nuclear modification of parton distributions.

Many models have been developed to simulate parton production based on Eq. (1) [8, 9, 10, 11]. In particular, HIJING and PCM have applied the techniques of renormalization group improved perturbative QCD, initially developed to study jet formation in e^+e^- and $p\bar{p}$ collisions [12, 13], to simulate initial and final state radiations associated with hard or semihard parton scatterings. Shown in Fig. 1 are the rapidity densities of produced partons given by HIJING and PCM [14]. Both models predict a large number of produced partons which will form a dense partonic gas as the initial condition immediately after the overlap of the two colliding nuclei with formation time, $1/p_T \sim 0.2$ fm/c. To ensure the credibility of these predictions, all models have been checked against the existing data of pp and $p\bar{p}$ collisions. It has been demonstrated that many aspects of multi-particle

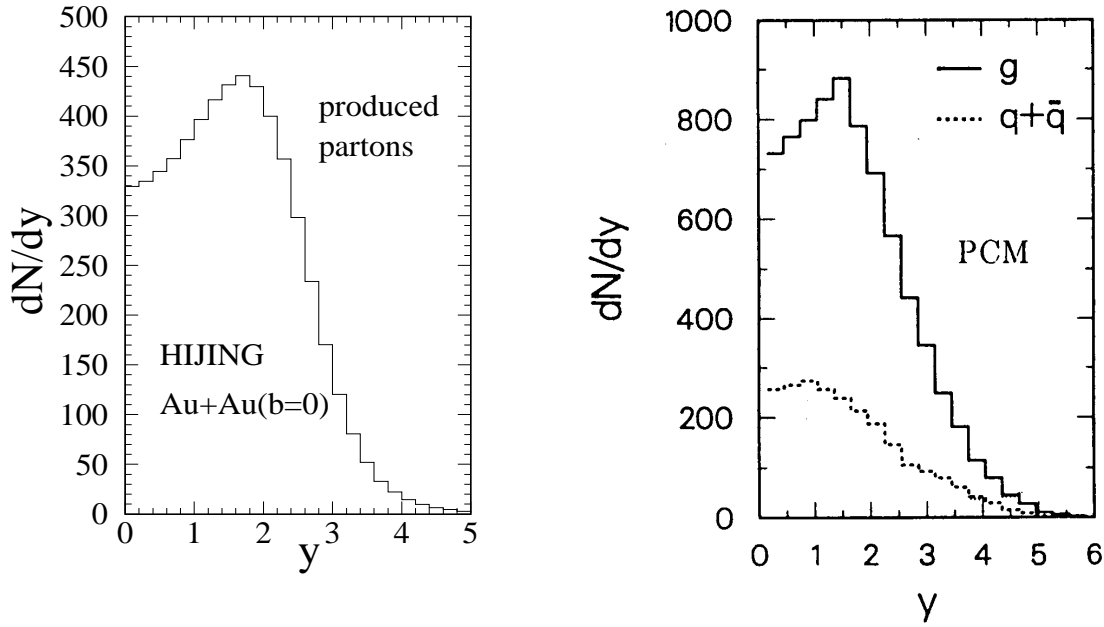


Figure 1. Rapidity distributions of produced partons given by HIJING and PCM calculations for central $Au + Au$ collisions at RHIC energy

production in pp and $p\bar{p}$ collisions can be accounted for by the onset of semihard parton scatterings in high energy hadronic collisions.

Even though existing pp and $p\bar{p}$ data can provide many constraints on these pQCD motivated phenomenological models, they still cannot uniquely determine all the parameters, giving rise to many uncertainties in the initial parton production:

(1) To regulate the infrared divergences in the QCD cross section of minijet production, a p_T cut-off p_0 has to be introduced. This cut-off and the corresponding soft inclusive cross section σ_{soft} for interactions with smaller $p_T < p_0$ are constrained by the energy dependence of the total pp and $p\bar{p}$ cross sections. These two parameters cannot be determined uniquely from the phenomenology of currently measured observables [15]. To reduce the uncertainties, measurement of two-particle correlation functions in azimuthal angle in the transverse plane was proposed [16] to further constrain p_0 and σ_{soft} .

(2) Since most of produced partons are gluons, their number is sensitive to the gluon distribution function $f_g(x)$ at small x . So far there is still no precise measurement of the gluon distribution function in the small x region where most of the minijets originate at RHIC and LHC energies. Though there have been theoretical attempts to study gluon distribution in a nucleus [17, 18], there is no direct experimental measurement of nuclear shadowing of the gluon distribution. Future experiments at HERA might provide information on the gluon distribution. In addition systematical measurements of pp , pA and AA interactions at RHIC can be used to study gluon shadowing [19].

(3) The treatment of primary-secondary parton scatterings can also lead to differences in the initial parton production. Because of formation time effect which I will discuss later,

Table 1

Values of the relevant parameters characterizing the parton gas at time τ_{iso} .

	RHIC	LHC
τ_{iso} (fm/c)	0.7	0.5
ε_0 (GeV/fm ³)	3.2	40
n_0 (fm ⁻³)	2.15	18
$\langle k_{\perp} \rangle$ (GeV)	1.17	1.76
T_0 (GeV)	0.55	0.82
λ_g^0	0.05	0.124
λ_q^0	0.008	0.02

most of the produced partons have no time to rescatter again with another oncoming beam parton before they pass through. Proper inclusion of such formation time effect will suppress primary-secondary parton scatterings [20, 21]. Systematic studies of pA collisions at RHIC will provide a quantitative estimate of this formation time effect.

(4) Finally, parton production from soft processes is also very model dependent. In parton cascade model, soft interactions are treated as elastic parton scatterings with a regularized distribution at small p_T . Such soft interactions with large cross section σ_{soft} can lead to many produced partons, especially when the long interaction time is not taken into account. In models with a string phenomenology, it is argued that soft interactions, though not calculable in pQCD, produce coherent gluons which form strings between leading partons. These strings can materialize into soft partons but at rather longer time scale of more than 1 fm/c. Color screening by the hard partons produced earlier can also reduce the soft parton production from the coherent color field [22].

3. EARLY PARTON DYNAMICS

The formation time of parton production can be estimated via uncertainty principle. Thus model calculations can also give the space-time history of parton production. Not surprisingly, it is found [20] that most of partons are produced within 0.4 fm/c after the complete overlap of two colliding nuclei. The parton system will then undergo further interactions and free-streaming. Neglecting parton rescatterings in this period of time, the kinematic separation of partons with different rapidities in a cell establishes local momentum isotropy at the time of the order of τ_{iso} [20, 23]. Given this initial time τ_{iso} , the parton rapidity density dN/dy and the average transverse momentum $\langle k_T \rangle$, the initial parton number and energy density can be estimated via Bjorken formula,

$$n_0 = \frac{1}{\pi R_A^2 \tau_{\text{iso}}} \frac{dN}{dy}, \quad \varepsilon_0 = n_0 \frac{4}{\pi} \langle k_T \rangle. \quad (3)$$

Assuming further that the phase distributions have a factorized form, $f_i(k) = \lambda_i f_{\text{eq}}(k, T)$, one can then estimate the effective initial temperature and fugacities. Listed in Table 1 are the initial conditions for central $Au + Au$ collisions at RHIC and LHC collider energies from HIJING calculations.

One can observe that the initial parton gas is rather hot reflecting the large average transverse momentum. However, the parton gas is still undersaturated as compared to the ideal gas at the same temperature. The gas is also dominated by gluons with its quark content far below the chemical equilibrium value, confirming the hot glue scenario [24].

How this parton gas evolves toward equilibrium is under intense investigation in the last few years. Tremendous progresses have been made with different approaches. Parton cascade model looks particularly interesting since it can provide a space-time picture of the evolution toward a thermalized quark-gluon plasma. Because of the classical nature of the cascade model, however, it is rather difficult to simulate many subtle quantum interference effects which are expected to be very important. For example, M. Gyulassy and I have studied the criteria for a semiclassical treatment of multiple parton scatterings. We found [25] that the billiard ball picture of multiple scatterings in a cascade model is valid only when the momentum transfer of each scattering is large enough to resolve the spatial separation of nearby scatterers which may not be true in the initial scatterings of the beam partons. Another important problem is the color interference in QCD and how it can be incorporated into semiclassical simulations.

The importance of color interference can be best demonstrated by comparing induced radiation in QED and QCD by a single scattering. In QED case, the radiation amplitude can be separated into initial state and final state radiation in the soft radiation limit,

$$\mathcal{R}_1 = ie \left(\frac{\epsilon \cdot p_i}{k \cdot p_i} - \frac{\epsilon \cdot p_f}{k \cdot p_f} \right), \quad (4)$$

where k and ϵ are the momentum and polarization of the radiated photon, respectively, p_i and p_f are the initial and final momentum of the charged particle. In the high energy limit, the two terms in \mathcal{R}_1 cancel to the order $\mathcal{O}(1/\sqrt{s})$ in the central region due to the destructive interference between initial and final state radiations. This gives rise to a valley in the photon's rapidity distribution as illustrated in Fig. 2(a). However, the cancellation will not be complete in QCD because gluons from initial and final state radiations have different colors due to the color exchange in the scattering. Furthermore, a gluon can also be emitted from the gluon propagator via the three gluon vertex. The resultant gluon spectrum [26],

$$\frac{dn_g}{dyd^2k_\perp} = \frac{C_A \alpha_s}{\pi^2} \frac{q_\perp^2}{k_\perp^2 (\mathbf{q}_\perp - \mathbf{k}_\perp)^2}. \quad (5)$$

has a plateau in the central rapidity region, as shown in Fig. 2(b). This is very different from the QED case.

Similarly, destructive interference between induced radiations by neighboring scatterings is also important. The radiation amplitude induced by multiple scatterings in QED, for example, is,

$$\mathcal{R}_m = ie \sum_{i=1}^m e^{ik \cdot x_i} \left(\frac{\epsilon \cdot p_i}{k \cdot p_i} - \frac{\epsilon \cdot p_{i-1}}{k \cdot p_{i-1}} \right). \quad (6)$$

In the eikonal limit (particle propagating along a straight line), the phase difference between any two terms can be written as,

$$k \cdot (x_i - x_j) = L_{ij}/\tau(k); \quad \tau(k) = \frac{1}{\omega(1 - \cos \theta)} \simeq \frac{2\omega}{k_\perp^2}, \quad (7)$$

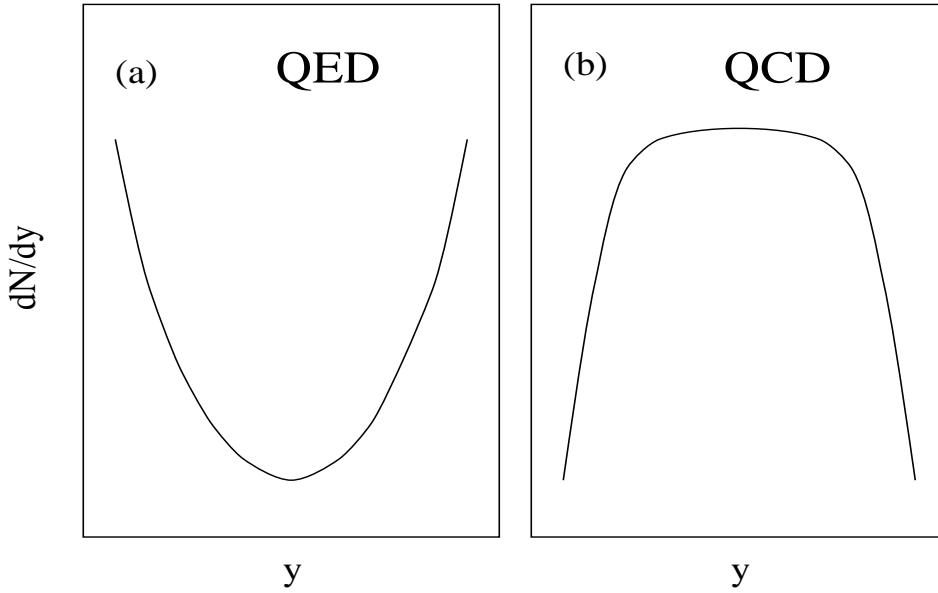


Figure 2. Illustrations of radiation spectrum in (a) QED and (b) QCD induced by a single scattering.

where L_{ij} is the distance (time) between scattering i and j , and $\tau(k)$ is the effective formation time. In the Bethe-Heitler limit $L_{ij} \gg \tau(k)$, the total intensity of induced radiation is simply additive in the number of scatterings. However, when $L_{ij} \ll \tau(k)$, the final state radiation of a scattering completely cancels with the initial state radiation from the previous one. This so-called Landau-Pomeranchuk-Migdal (LPM) effect can also be understood in terms of uncertainty principle: A radiated photon (or gluon in QCD) must travel at least one wavelength $1/k_{\perp}$ in the transverse direction in order to be separated from its parent particle. The radiation will be suppressed if the parent particle suffers another scattering within time (distance) $\tau(k)$, leading to the LPM effect.

Analysis in QCD gives similar results, although one has to take into account different color structures associated with different scatterings. In Ref. [25], M. Gyulassy and I considered induced radiation by multiple scatterings in the soft radiation limit and neglected the situation where a radiated gluon can suffer further interactions. We obtained a suppressed gluon spectrum with effective formation time,

$$\tau_{\text{QCD}}(k) = \frac{C_A}{2C_2} \tau(k). \quad (8)$$

Baier *et al.* [27] recently argued that those diagrams which were neglected in Ref. [25] might be important especially when a radiated real gluon travels with the beam particle for a long time and then is knocked off later. This argument will have important consequences in the energy loss of a fast parton propagating in a QCD medium [28]. However, I will use the above analysis in terms of effective formation time to discuss induced radiation in the context of parton equilibration.

4. PARTON EQUILIBRATION RATE

I would like to emphasize that the above interference effects happen on the matrix elements level. In particular, the LPM effect involves the interference between initial and final state radiations from different scatterings. A detailed analysis [25, 28] can show that the interference actually happens between two amplitudes in which the beam parton has completely different virtualities, *i.e.*, time-like in the final state radiation of one scattering and space-like in the initial state radiation of the previous one. This imposes a great difficulty for a proper treatment of the quantum interference in a parton cascade model in which a parton must *always* remain time-like between two scatterings [9]. A possible remedy for this is to consider both initial and final state radiation associated with each scattering together and include the interference effect by using a modified radiation spectrum. The effective spectrum should suppress soft gluon radiation whose formation time is larger than the mean-free-path of parton scatterings. To demonstrate this, let us consider parton equilibration in the form of rate equations [23]. The analysis of QCD LPM effect [25, 28] has been done for a fast parton traveling inside a parton plasma. I will apply the results to radiations off thermal partons whose average energy is about T , since we expect the same physics to happen.

We consider only the dominant process $gg \rightarrow ggg$ in the leading order. In order to permit the approach to chemical equilibrium, the reverse process, *i.e.*, gluon absorption, has to be included as well, which is easily achieved making use of detailed balance. Radiative processes involving quarks have substantially smaller cross sections in pQCD, and quarks are considerably less abundant than gluons in the initial phase of the chemical evolution of the parton gas. Here we are interested in understanding the basic mechanism underlying the formation of a chemically equilibrated quark-gluon plasma, and the essential time-scale. We hence restrict our considerations to the dominant reaction mechanism for the equilibration of each parton flavor. These are just four processes:

$$gg \leftrightarrow ggg, \quad gg \leftrightarrow q\bar{q}. \quad (9)$$

Other scattering processes ensure the maintenance of thermal equilibrium ($gg \leftrightarrow gg$, $gq \leftrightarrow gq$, etc.) or yield corrections to the dominant reaction rates ($gq \leftrightarrow qgg$, etc.).

Restricting to the above reactions and assuming that elastic parton scatterings are sufficiently rapid to maintain local thermal equilibrium, the evolution of the parton densities is governed by the master equations [23]:

$$\partial_\mu(n_g u^\mu) = \frac{1}{2}\sigma_3 n_g^2 \left(1 - \frac{n_g}{\tilde{n}_g}\right) - \frac{1}{2}\sigma_2 n_g^2 \left(1 - \frac{n_q^2 \tilde{n}_g^2}{\tilde{n}_q^2 n_g^2}\right), \quad (10)$$

$$\partial_\mu(n_q u^\mu) = \frac{1}{2}\sigma_2 n_g^2 \left(1 - \frac{n_q^2 \tilde{n}_g^2}{\tilde{n}_q^2 n_g^2}\right), \quad (11)$$

where $\tilde{n}_i \equiv n_i/\lambda_i$ denote the densities with unit fugacities, $\lambda_i = 1$, σ_3 and σ_2 are thermally averaged, velocity weighted cross sections,

$$\sigma_3 = \langle \sigma(gg \rightarrow ggg)v \rangle, \quad \sigma_2 = \langle \sigma(gg \rightarrow q\bar{q})v \rangle. \quad (12)$$

We have also assumed detailed balance and a baryon symmetric matter, $n_q = n_{\bar{q}}$. If we

neglect effects of viscosity due to elastic scattering [29], we then have the hydrodynamic equation

$$\frac{d\varepsilon}{d\tau} + \frac{\varepsilon + P}{\tau} = 0. \quad (13)$$

We further assume the ultrarelativistic equation of motion, $\varepsilon = 3P$. We can then solve the hydrodynamic equation,

$$[\lambda_g + \frac{b_2}{a_2}\lambda_q]^{3/4}T^3\tau = \text{const.} \quad , \quad (14)$$

and rewrite the rate equation in terms of time evolution of the parameters $T(\tau)$, $\lambda_g(\tau)$ and $\lambda_q(\tau)$,

$$\frac{\dot{\lambda}_g}{\lambda_g} + 3\frac{\dot{T}}{T} + \frac{1}{\tau} = R_3(1 - \lambda_g) - 2R_2\left(1 - \frac{\lambda_q^2}{\lambda_g^2}\right) \quad (15)$$

$$\frac{\dot{\lambda}_q}{\lambda_q} + 3\frac{\dot{T}}{T} + \frac{1}{\tau} = R_2\frac{a_1}{b_1}\left(\frac{\lambda_g}{\lambda_q} - \frac{\lambda_q}{\lambda_g}\right), \quad (16)$$

where the density weighted reaction rates R_3 and R_2 are defined as

$$R_3 = \frac{1}{2}\sigma_3 n_g, \quad R_2 = \frac{1}{2}\sigma_2 n_g. \quad (17)$$

Notice that for a fully equilibrated system ($\lambda_g = \lambda_q = 1$), Eq. (14) corresponds to the Bjorken solution, $T(\tau)/T_0 = (\tau_0/\tau)^{1/3}$.

To take into account of the LPM effect in the calculation of the reaction rate R_3 for $gg \rightarrow ggg$, we simply impose the LPM suppression of the gluon radiation whose effective formation time τ_{QCD} is much longer than the mean-free-path λ_f of multiple scatterings to each $gg \rightarrow ggg$ process. In the mean time, the LPM effect also regularizes the infrared divergency associated with QCD radiation. However, σ_3 still contains infrared singularities in the gluon propagators. For an equilibrium system one can in principle apply the resummation technique developed by Braaten and Pisarski [30] to regularize the electric part of the propagators, though the magnetic sector still has to be determined by an unknown magnetic screening mass. Since we are dealing with a nonequilibrium system, Braaten and Pisarski's resummation may not be well defined. As an approximation, we will use the Debye screening mass [31],

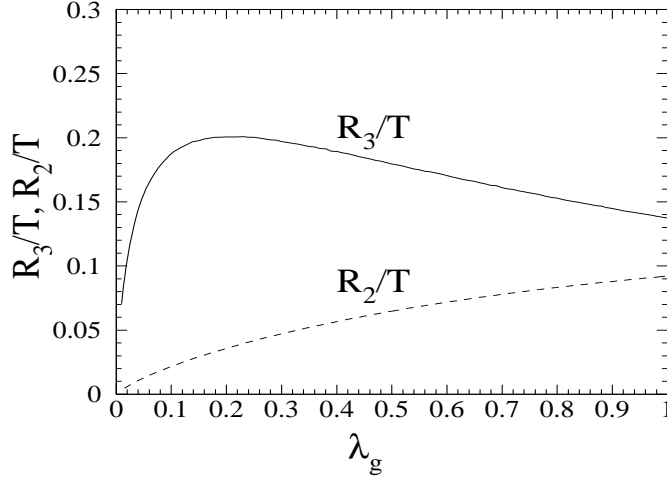
$$\mu_D^2 = \frac{6g^2}{\pi^2} \int_0^\infty k f(k) dk = 4\pi\alpha_s T^2 \lambda_g, \quad (18)$$

to regularize all singularities in the radiative cross section.

To further simplify the calculation we approximate the LPM suppression factor in Ref. [25, 28] by a θ -function, $\theta(\lambda_f - \tau_{\text{QCD}})$. The modified differential cross section for $gg \rightarrow ggg$ is then,

$$\frac{d\sigma_3}{dq_\perp^2 dy d^2k_\perp} = \frac{d\sigma_{\text{el}}^{gg}}{dq_\perp^2} \frac{dn_g}{dy d^2k_\perp} \theta(\lambda_f - \tau_{\text{QCD}}) \theta(\sqrt{s} - k_\perp \cosh y), \quad (19)$$

Figure 3. The scaled gluon production rate R_3/T (solid line) for $gg \rightarrow ggg$ and the quark production rate R_2/T (dashed line) for $gg \rightarrow q\bar{q}$ as functions of the gluon fugacity λ_g for $\alpha_s = 0.3$.



where the second step-function accounts for energy conservation, and $s = 18T^2$ is the average squared center-of-mass energy of two gluons in a thermal gas. The regularized gluon density distribution induced by a single scattering is,

$$\frac{dn_g}{dyd^2k_\perp} = \frac{C_A\alpha_s}{\pi^2} \frac{q_\perp^2}{k_\perp^2[(\mathbf{k}_\perp - \mathbf{q}_\perp)^2 + \mu_D^2]}. \quad (20)$$

Similarly, the regularized small angle gg scattering cross is,

$$\frac{d\sigma_{\text{el}}^{gg}}{dq_\perp^2} = \frac{9}{4} \frac{2\pi\alpha_s^2}{(q_\perp^2 + \mu_D^2)^2}. \quad (21)$$

The mean-free-path for elastic scatterings is then,

$$\lambda_f^{-1} \equiv n_g \int_0^{s/4} dq_\perp^2 \frac{d\sigma_{\text{el}}^{gg}}{dq_\perp^2} = \frac{9}{8} a_1 \alpha_s T \frac{1}{1 + 8\pi\alpha_s\lambda_g/9}, \quad (22)$$

which depends very weakly on the gluon fugacity λ_g .

We can evaluate the integration numerically and find out the dependence of R_3/T on the gluon fugacity λ_g as shown in Fig. 3, for a coupling constant $\alpha_s = 0.3$. The gluon production rate increases with λ_g and then saturates when the system is in equilibrium. Overall, the gluon equilibration rate is suppressed due to the inclusion of the LPM effect on induced radiation.

The calculation of the quark equilibration rate R_2 for $gg \rightarrow q\bar{q}$ is more straightforward. Estimate in Ref. [23] gives,

$$R_2 = \frac{1}{2} \sigma_2 n_g \approx 0.24 N_f \alpha_s^2 \lambda_g T \ln(5.5/\lambda_g). \quad (23)$$

The dashed line in Fig. 3 shows the normalized rate R_2/T for $N_f = 2.5$, taking into account the reduced phase space of strange quarks at moderate temperatures, as a function of the gluon fugacity.

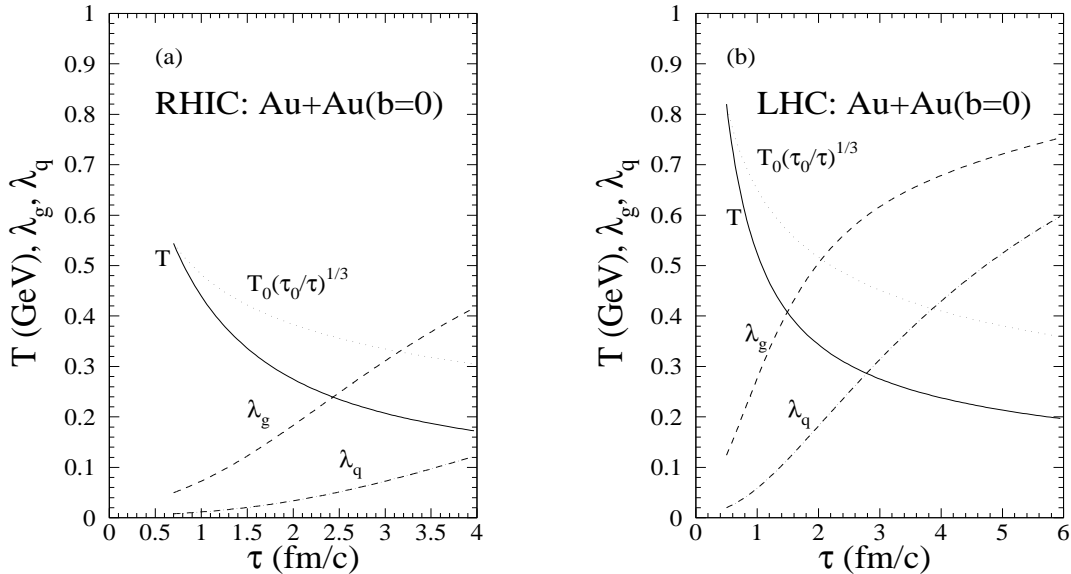


Figure 4. Time evolution of the temperature T and the fugacities λ_g and λ_q of gluons and quarks in the parton plasma for central $Au + Au$ collisions at the (a) RHIC and (b) LHC energies. The initial values for T , λ_g and λ_q are determined from HIJING simulations and are listed in Table 1.

5. EVOLUTION OF THE PARTON PLASMA

With the parton equilibration rates which in turn depend on the gluon fugacity, we can solve the master equations self-consistently and obtain the time evolution of the temperature and the fugacities. Shown in Fig. 4 is the time dependence of T , λ_g , and λ_q for initial conditions listed in Table 1 at the RHIC and LHC energies. We find that the parton gas cools considerably faster than predicted by Bjorken's scaling solution ($T^3\tau = \text{const.}$) shown as dotted lines, because the production of additional partons approaching the chemical equilibrium state consumes an appreciable amount of energy. The accelerated cooling, in turn, slows down the chemical equilibration process, which is more apparent at the RHIC than at LHC energies. Therefore, the parton system can hardly reach its equilibrium state before the effective temperature drops below $T_c \approx 200$ MeV in a short period of time of 1-2 fm/c at the RHIC energy. At the LHC energy, however, the parton gas becomes very close to its equilibrium and the plasma may exist in a deconfined phase for as long as 4-5 fm/c. Another important observation is that quarks never reach chemical equilibrium at both energies. This is partially due to the small initial quark fugacity and partially due to the small quark equilibration rate.

In another recent development, E. Shuryak and L. Xiong [32] used the complete matrix elements of $gg \rightarrow gg + (n - 1)g$ which include complete interference to calculate the parton equilibration rate. This is essentially a step beyond leading logarithmic approximation used in most of the calculations. They found that inclusion of these higher order corrections not only increases the initial parton production but also the parton equilibra-

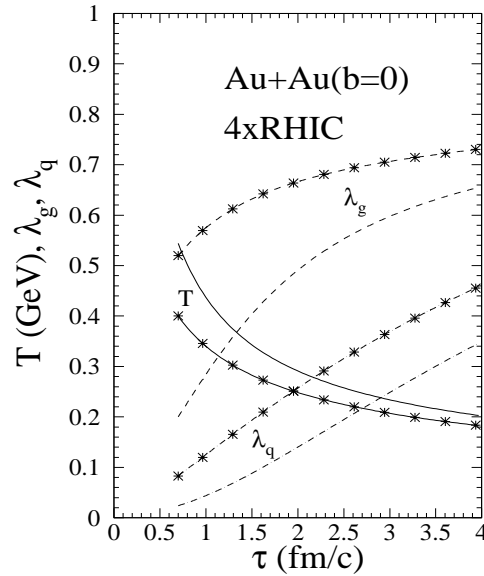


Figure 5. The same as in Fig. 4(a), except that the initial parton densities are 4 times higher than given in Table 1 with the same (ordinary lines), or reduced initial temperature, $T_0 = 0.4$ GeV (lines with stars)

tion rate. However, it is expected that if the formation time and virtual corrections (or unitarity) are included in this multiple gluon radiation processes, the effect could become smaller.

As I have pointed out, there are still a lot of uncertainties in the initial parton production. We can estimate the effect of the uncertainties in the initial conditions on the parton gas evolution by multiplying the initial energy and parton number densities at the RHIC energy by a factor of 4. This will result in the initial fugacities, $\lambda_g^0 = 0.2$ and $\lambda_q^0 = 0.024$. With these high initial densities, the parton plasma can evolve into a nearly equilibrated gluon gas as shown in Fig. 5. The deconfined phase will also last longer for about 4 fm/c. The system is still dominated by gluons with few quarks and antiquarks as compared to a chemically equilibrated system. If the uncertainties in the initial conditions are caused by soft parton production from the color mean field, the initial effective temperature will decrease. Therefore, we can alternatively increase the initial parton density by a factor of 4 and decrease T_0 to 0.4 GeV at the same time. This leads to higher initial fugacities, $\lambda_g^0 = 0.52$ and $\lambda_q^0 = 0.083$. As shown in Fig. 5 by the curves with stars, this system evolves faster toward equilibrium, however, with shorter life-time in the deconfined phase due to the reduced initial temperature.

We thus can conclude that perturbative parton production and scatterings are very likely to produce a quark-gluon plasma (or more specifically a gluon plasma) in ultra-relativistic heavy ion collisions at the RHIC and LHC energies. However, uncertainties in the initial conditions have to be carefully examined in order to give a definite prediction of the quark-gluon plasma at the RHIC energy.

6. PROBES OF EARLY PARTON DYNAMICS

While some of the uncertainties may be reduced by theoretical studies of the parton distribution in nuclei and initial parton production, most of them have to be resolved experimentally. There are many processes the measurements of which can provide experimental probes of the early parton dynamics. For example, suppression of large p_T jet or jet quenching [19, 33, 34, 35] due to the final state interaction of large p_T parton with the parton gas can be used to study parton equilibration in the early stage. Furthermore, the energy loss of the jets and the acoplanarity [36, 37] can also be used to study the thermal dynamical properties of the parton gas .

Among these hard probes, electromagnetical signals like thermal photons and dileptons are considered more direct since they can escape the dense matter without further interactions. They can thus reveal the dynamics of initial parton production and equilibration. In addition, open charm production can also be considered as a direct probe since charm quarks cannot be easily produced during the mixed and hadronic phases of the dense matter due to their heavy masses. To leading order in pQCD, dilepton production is dominated by $q\bar{q} \rightarrow \ell^+\ell^-$, direct photon by $q(\bar{q})g \rightarrow q(\bar{q})\gamma$ and open charm by $gg \rightarrow c\bar{c}$ processes. As pointed out by Strickland [38], measurements of these direct thermal signals can tell us the relative ratio of quark and gluon number densities in the early stage of parton equilibration.

To demonstrate the sensitivity of these direct probes to the initial condition of the parton evolution, let us consider open charm production as an example. Charm production can be divided into three different contributions in the history of the evolution of the parton system: (1) initial production during the overlapping period ; (2) pre-thermal production from secondary parton scatterings during the thermalization, $\tau < \tau_{\text{iso}}$; (3) and thermal production during the parton equilibration, $\tau > \tau_{\text{iso}}$, in the expanding system. The initial charm production can be calculated similarly to minijet production [cf. Eq. (1)]. For thermal and pre-thermal production, the differential rate is[39],

$$E \frac{d^3 A}{d^3 p} = \frac{1}{16(2\pi)^8} \int \frac{d^3 k_1}{\omega_1} \frac{d^3 k_2}{\omega_2} \frac{d^3 p_2}{E_2} \delta^{(4)}(k_1 + k_2 - p - p_2) \left[\frac{1}{2} g_G^2 f_g(k_1) f_g(k_2) |\overline{\mathcal{M}}_{gg \rightarrow c\bar{c}}|^2 + g_q^2 f_q(k_1) f_{\bar{q}}(k_2) |\overline{\mathcal{M}}_{q\bar{q} \rightarrow c\bar{c}}|^2 \right], \quad (24)$$

given the phase-space density of the equilibrating partons, $f_i(k)$, where $g_G=16$, $g_q = 6N_f$, are the degeneracy factors for gluons and quarks (antiquarks) respectively, $|\overline{\mathcal{M}}_{gg \rightarrow c\bar{c}}|^2$, $|\overline{\mathcal{M}}_{q\bar{q} \rightarrow c\bar{c}}|^2$ are the *averaged* matrix elements for $gg \rightarrow c\bar{c}$ and $q\bar{q} \rightarrow c\bar{c}$ processes. Due to small charm density, the Pauli blocking of the final charm quarks can be neglected. The corresponding charm spectrum is

$$\frac{dN_c}{dy d^2 p_\perp} = \pi R_A^2 \int d\eta d\tau E \frac{d^3 A}{d^3 p}. \quad (25)$$

For pre-thermal charm production, one can use the momentum spectrum of initially produced partons and model the phase distribution by introducing a correlation between momentum and space-time. This correlation was shown to be important in the calculation of pre-thermal charm production [40, 41]. For thermal production, one can use the time

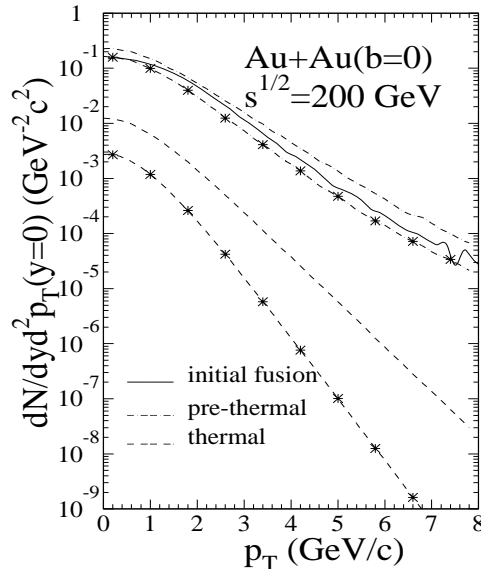


Figure 6. The p_{\perp} distribution of the initial (solid), pre-thermal (dot-dashed) and thermal (dashed) charm production for initial parton densities 4 times higher than HIJING estimate given in 1 but with the same (ordinary lines), or reduced initial temperature, $T_0 = 0.4$ GeV (lines with stars).

dependence of temperature and fugacities as given by the parton evolution equations. Shown in Fig. 6 are the charm production rates as functions of p_T with the same initial conditions in Fig. 5. Note that with the increased initial parton density, open charm production from pre-thermal and thermal stage is as important as the initial production. Thermal production is more sensitive to the variation of the initial temperature than the initial fugacities. Therefore, by measuring charm enhancement, we can probe the initial parton phase-space distribution, initial temperature and equilibration time.

7. CONCLUSIONS

In this talk I reviewed the pQCD-based models of ultrarelativistic heavy ion collisions. In this framework the reaction dynamics can be described by perturbative parton scatterings and radiations. Using model estimate of initial parton production, it is found that there are enormous number of partons produced during the overlap period of two colliding nuclei. Thereafter, local isotropy in momentum distribution might be reached. Parton proliferation through induced radiation and parton fusion further drive the parton system toward a fully equilibrated parton plasma. The quarks always lag behind gluons in reaching their equilibrium. Due to the energy consumption by parton production, the parton gas cools down faster leading to a reduced plasma life time of 4 - 6 fm/c.

Throughout the production and evolution of the partonic system, interference effects play an important role in multiple collisions, the correct implementation of which will be a great challenge to any *classical* cascade models. Especially, the destructive interference among different amplitudes of gluon radiation induced by multiple scatterings suppresses

soft gluons whose formation time is larger than the mean-free-path of parton scatterings inside a QCD medium. A detailed analysis of the radiation amplitudes reveals the underlying physics which contradicts the intuitive picture of a classical cascade model. One way to incorporate the LPM effect in the parton interaction simulations is to consider both the initial and final state radiation together for each scattering and impose the formation time requirement, $\tau_{\text{QCD}} < \lambda_f$, for the integration over the phase-space of the radiated gluons. This will lead to a reduced parton equilibration rate.

I also discussed the uncertainties in the initial conditions and the experimental probes of the early parton evolution. All in all, these uncertainties arise from our ignorance of the nonperturbative physics and our inability to calculate the soft processes in the framework of QCD. In the pQCD-based models I have reviewed here, the uncertainties really lie in the cut-off, p_0 , which supposes to separate nonperturbative soft interactions from perturbative hard processes. Since soft and hard physics do not have a definite boundary, the resultant parton production from hard or semihard is very sensitive to the cut-off. The accompanying soft parton production is not known in this model and may only be estimated by simple models like the color flux-tube model [22]. There have been recent developments in the field theory of particle production from mean-fields [42, 43]. The chaotic behavior of nonabelian gauge fields may be intimately related to multiple parton production and fast gluon equilibration [44]. Such a field theoretical approach to particle production could be the ultimate and consistent way to address the production and formation of a parton plasma in heavy ion collisions.

In conclusion, parton equilibration is an exciting new subject with many unsolved problems. I hope eventually, not far from now, we can explicitly explain whether and how a quark-gluon plasma is formed in a heavy ion collisions.

Acknowledgements I would like to thank my collaborators T. S. Biró, K. J. Eskola, M. Gyulassy, P. Lévai, B. Müller and M. H. Thoma who made significant contributions to the work I reviewed in this talk. Stimulating discussions with M. Asakawa, K. Geiger, H. Heiselberg, J. I. Kapusta, L. McLerran, E. Shuryak, and L. Xiong are also gratefully acknowledged.

REFERENCES

- [1] K. Geiger, Nucl. Phys. **A566**, 257c (1994), in Quark Matter'93, Proceedings of the 10th International Conference on Ultrarelativistic Nucleus-Nucleus Collisions, Borlänge, Sweden, June 20, 1993, edited by E. Stenlund, H.-Å. Gustafsson, A. Oskarsson and I. Otterlund.
- [2] H. H. Gutbrod, A. M. Poskanzer and H. G. Ritter, Rep. Prog. Phys. **52**, 267 (1989).
- [3] J. Barrette *et al.*, Phys. Rev. Lett. **73**, 2532 (1994).
- [4] X.-N. Wang and M. Gyulassy, Phys. Rev. D **45**, 844 (1992).
- [5] J. P. Blaizot and A. H. Mueller, Nucl. Phys. **B289**, 847 (1987).
- [6] K. Kajantie, P. V. Landshoff, and Lindfors, Phys. Rev. Lett. **59**, 2527 (1987); K. J. Eskola, K. Kajantie and J. Lindfors, Nucl. Phys. **B323**, 37 (1989).
- [7] G. Altarelli and G. Parisi, Nucl. Phys. **B126**, 298 (1977).
- [8] X.-N. Wang and M. Gyulassy, Phys. Rev. D **44**, 3501 (1991); Comp. Phys. Commun. **83**, 307 (1994).

- [9] K. Geiger and B. Müller, Nucl. Phys. **B369**, 600(1992); K. Geiger, Phys. Rev. D **47**, 133 (1993).
- [10] N. S. Amelin, E. F. Staubo, L. P. Csernai, Phys. Rev. D **46**, 4873 (1992).
- [11] I. Kawrakov, H.J. Mohring and J. Ranft, Phys. Rev. D **47**, 3849 (1993).
- [12] G. Marchesini and B. R. Webber, Nucl. Phys. **B238**, 1 (1984).
- [13] T. Sjostrand and M. van Zijl, Phys. Rev. D **36**, 2019 (1987).
- [14] K. Geiger and J. I. Kapusta, Phys. Rev. D **47**, 4905 (1992).
- [15] X.-N. Wang, Phys. Rev. D **43**, 104 (1991).
- [16] X.-N. Wang, Phys. Rev. D **46**, R1900 (1992), Phys. Rev. D **47**, 2754 (1993).
- [17] K. J. Eskola, J. Qiu and X.-N. Wang, Phys. Rev. Lett. **72**, 36 (1994).
- [18] L. McLerran and R. Venugopalan, Phys. Rev. D **49**, 3352 (1994).
- [19] X.-N. Wang and M. Gyulassy, Phys. Rev. Lett. **68**, 1480 (1992).
- [20] K. J. Eskola and X.-N. Wang, Phys. Rev. D **49**, 1284 (1994).
- [21] X.-N. Wang, in proceedings of the Workshop on Finite Temperature QCD and Quark-gluon Transport Theory, Wuhan, China, April 18-26, 1994, edited by Lianshou Liu (World Scientific).
- [22] K. J. Eskola and M. Gyulassy, Phys. C **47**, 2329 (1993).
- [23] T. S. Biró, E. van Doorn, B. Müller, M. H. Thoma, and X.-N. Wang, Phys. Rev. C **48**, 1275 (1993).
- [24] E. Shuryak, Phys. Rev. Lett. **68**, 3270 (1992).
- [25] M. Gyulassy and X.-N. Wang, Nucl. Phys. **B420**, 583 (1994).
- [26] J. F. Gunion and G. Bertsch, Phys. Rev. D **25**, 746 (1982).
- [27] R. Baier, Yu. L. Dokshitzer, S. Peigné and D. Schiff, Report LPTHE-Orsay 94/98.
- [28] X.-N. Wang, M. Gyulassy and M. Plümer, LBL-35980, Phys. Rev. D in press.
- [29] P. Danielewicz and M. Gyulassy, Phys. Rev. D **31**, 53 (1985); A. Hosoya and K. Kajantie, Nucl. Phys. **B250**, 666 (1985); S. Gavin, Nucl. Phys. **A435**, 826 (1985).
- [30] E. Braaten and R. D. Pisarski, Nucl. Phys. **B337**, 569 (1990).
- [31] T. S. Biró, B. Müller, and X.-N. Wang, Phys. Lett. **B283**, 171 (1992).
- [32] L. Xiong and E. Shuryak, Phys. Rev. C **49**, 2207 (1994).
- [33] M. Gyulassy and M. Plümer, Phys. Lett. **B243**, 432 (1990).
- [34] M. Gyulassy, M. Plümer, M. H. Thoma and X.-N. Wang, Nucl. Phys. **A538**, 37c (1992).
- [35] M. Plümer, M. Gyulassy, X.-N. Wang, Proceedings of Quark Matter'95, Monterey, Jan. 9, 1995, edited by A. M. Poskanzer, J. W. Harris and L. S. Schroeder.
- [36] J.-C. Pan, C. Gale, Phys. Rev. D **50**, 3235 (1994).
- [37] S. Gupta, Report TIFR-TH-94-29, 1994.
- [38] M. T. Strickland, Phys. Lett. **B331**, 245 (1994).
- [39] B. Müller and X. N. Wang, Phys. Rev. Lett. **68**, 2437 (1992).
- [40] Z. Lin and M. Gyulassy, Report CU-TP-638.
- [41] P. Lévai, B. Müller and X.-N. Wang, Report LBL-36594.
- [42] Y. Kluger, J. M. Eisenberg, B. Svetisky, F. Cooper and E. Mottola, Phys. Rev. Lett. **67**, 2427 (1991); Phys. Rev. D **45**, 4659 (1992); *ibid.* D **48**, 190 (1993).
- [43] H.-T. Elze, CERN-TH-7131-93, hep-ph-9404215; CERN-TH-7297-94, hep-th-9406085.
- [44] B. Müller and A. Trayanov, Phys. Rev. Lett. **68**, 3387 (1992); C. Gong, S. G. Matinian, B. Müller and A. Trayanov, Phys. Rev. D **49**, 607 (1994), *ibid.* D **49**, 5629 (1994).